Hybrid Optimization with Recurrent Neural Network-based Medical Image Processing for Predicting Interstitial Lung Disease

K.Sundaramoorthy[1], R.Anitha[2], Dr.S.Kayalvili[3], Ayat Fawzy Ahmed Ghazala[4], Prof. Ts. Dr. Yousef A.Baker El-Ebiary[5], Sameh Al-Ashmawy[6]

Professor, Information Technology, Jerusalem College of Engineering, Velachery Road, Narayanapuram, Pallikaranai, Chennai-600100[1]

Professor, Biomedical Engineering, Jerusalem College of Engineering, Velachery Road, Narayanapuram, Pallikaranai, Chennai-600100[2]

Professor, Department of Computer Science and Engineering, Velalar College of Engineering and Technology, Thindal, Erode - 638012. Tamil Nadu[3]

Assistant Professor, Department of Education and Psychology-College of Science and Arts in Al-Qurayyat, Jouf University - Saudi Arabia[4]

Assistant Professor Educational Technology - Faculty of Specific Education - Menoufia University – Egypt[4]

Faculty of Informatics and Computing, UniSZA University, Malaysia[5]

Imam AbdulRahman Bin Faisal University- Kingdom of Saudi Arabia[6]

***Abstract*—One of the dreadful diseases that shortens people's lives is lung disease. There are numerous potentially fatal consequences that can arise from interstitial lung disease, such as: Lung hypertension. This illness doesn't influence your overall blood pressure; instead, it only affects the arteries in your lungs. To prevent mortality, it is essential to accurately diagnose pulmonary illness in patients. Various classifiers, including SVM, RF, MLP, and others, are processed to identify lung disorders. Large datasets cannot be processed by these algorithms, which causes false lung disease identification. A combined new Spider Monkey and Lion algorithm is suggested as a solution to get around these limitations. Images of interstitial lung disease (ILD) were taken for the study from the publicly accessible MedGIFT database. The median filter is employed during the pre-processing step of ILD images to reduce noise and remove undesirable objects. The features are extracted using a hybrid spider Monkey and Lion algorithm. The lungs' damaged and unaffected regions are divided into categories using recurrent neural networks. Several metrics such as accuracy, precision, recall, and f1-score are used to evaluate the performance of the proposed system. The results demonstrate that this technique offers more precision, accuracy, and a higher rate of lung illness detection by processing a large number of computerized tomography representations quickly. When compared to other strategies already in use, the proposed model's accuracy is greater at 99.8%. This method could be beneficial for staging the severity of interstitial lung illness, prognosticating, and forecasting treatment outcomes and survival, determining risk control, and allocation of resources.**

Keywords*—Interstitial lung disease; spider monkey lion optimization; recurrent neural network; medical image processing; diagnosis and identification; classification

I. INTRODUCTION

In the U.S, lung disease is the most common cause of mortality. Lung disease affects the lives of over 400,000 Americans each year, and risk of death from this disease is rising even while they fall for other serious diseases like cancer. ILDs are a diverse group of more than 200 lung conditions that mostly affect the lung parenchyma but can also appear as respiratory or vascular symptoms. Numerous lung conditions, including interstitial lung disease, chronic obstructive pulmonary disease, and acute respiratory distress syndrome, are linked to the mechanical performance of the lung. ILD is a group of devastating disorders where fibrosis damages and stiffens lung tissue [1].

A class of extensive parenchymal lung ailments known as "interstitial lung diseases" are highly diseased and lethal. The establishment of a new categorization of idiopathic interstitial respiratory infections, which divides the condition into three categories—major, uncommon, and unclassified [2]. The updated version is unusual because it allows for the treatment of threatening matters in accordance with the disease classification. Foremost fatal interstitial lung disease, idiopathic pulmonary fibrosis exhibits a great degree of symptomatic variability. The therapist managing the impacted patient faces a substantial problem when dealing with lLD in an apparently healthy host that seems to be ordinary. A comprehensive group of specialists should examine a mix of diagnostic, radiology, and abnormal criteria that are used to diagnose an ILD [3]. The pathophysiology of these disorders has been linked to a number of variables, including genetic component, diseases, medications, thermal energy, and workplace and environmental durations.

Idiopathic pulmonary fibrosis, sarcoidosis, hypersensitivity pneumonitis, ILD as a symptom of connective tissue disease, drug induced ILD, and pneumoconiosis are the most common types of ILD. The most prevalent and serious type of ILD, IPF, has drawn the considerable attention in respiratory research. Interstitial fibrosis, also known as the common

technique of UIP, is visible on HRCT of the lung in IPF patients. Compared to other respiratory problems, ILD have a stronger link to health hazards. The pneumoconiosis is caused by asbestosis, silicosis, and coal worker's pneumoconiosis is typical instances of industrial disorders [4].

Infection and fibrosis of the lung tissue characterise the category of lung disorders known as ILD and pulmonary fibrosis. IPF is a specific type of ILD, and because of its unidentified origin, poor overall outcome, and moderate reaction to clinical treatment, IPF is frequently regarded as one of the most prevalent and significant ILDs. Although the treatment for ILD and pulmonary fibrosis can occasionally be complicated, it is based on the ILD's most likely origin. Additionally, the outcomes of the medical evaluation, auto-immune serologic analysis, chest CT imaging, and, if necessary, a lung sample must be added to the health information in order to make a precise ILD classification [5]. PFTs are crucial for care and typically reveal a sequence of a restrictive ventilator disorder with an aberrant continues to prove, but they mostly serve as a gauge for the extent of the condition and its prognosis by identifying a particular type of ILD [6].

A record-breaking volume of data has been generated as a result of the enormous progress in image capture technology, capacity growth, and the installation of bio-medical information collection equipment [7]. These data come from numerous (sometimes inconsistent) database systems, have a high dimension (Computed tomography, Magnetic resonance imaging, etc.), and are rich in variables. It provides healthcare information that is difficult, particularly on images [8]. DL assists in creating new ones. In addition, DL not only aids in disease detection but also evaluates the predicted goal and gives proactive forecast models to help doctors create efficient treatment protocols. Every scientific subject, especially medical image into regions, is involved in DL. The usage of a DNN model is implied by the phrase DL [9]. Various samples are inputted into the NN, and combines with parameters to produce digital output through non-linear processes. The classification of ILD is given in Fig. 2.

One of the crucial components of digital image processing used for medical planning in healthcare systems is medical imaging. Additionally, a significant amount of medical data is employed in medical field for scientific and educational purposes, such as clinical data visualisation. For quicker distribution, the clinical images are reduced and kept hidden. Due to their smaller system memory, compressed images have an extremely short transmission rate[10]. Typically, there are two types of compression: both lossy and lossless methods. With file format, input images are offered without any losses, and the output image is identical to the original image. However, compression ratio offers a lower compression ratio [11]. FFNN, which has loops in the hidden units, is often enhanced by recurrent neural network (RNN). It is capable of learning combinations. All stages and neurotransmitters share the same weights. The framework provides the model to take sample segments as input and determines the temporal link between the data. The representation of dynamical modification at a time series is handled using this Classifier [12].

The following criteria contribute identify interstitial lung disease:

- The research suggests the most appropriate deep-learning approach for identifying and classifying interstitial lung disease (ILD) from medical images.
- The dataset was gathered from patient medical images who had ILDs. The first scenario is pre-processing of medical images, the second is feature extraction and selection, and the third is categorization.
- The findings show that the proposed hybrid Spider Monkey and Lion algorithm has effectively selected the features and the deep learning-based recurrent neural network (RNN) is capable of recognizing the ILD classification.

The remaining part of this article has been organized as follows: Section II provides a detailed description of the most recent techniques for classifying interstitial lung disease. The dataset obtained from individuals with interstitial lung disease is described in Section III. Section IV covers the system structure and assessment method, which includes image pre-processing and the steps taken to develop the extraction of features for categorization. The findings and discussion sections are described in Section V accordingly. Lastly, Section VI presents the relevant outcomes of the study.

II. Related Works

In this paper [13] , a convolutional neural network for classifying ILD sequences is evaluated. The network is composed of three dense layers, an averaged pooling with a size equivalent to the length of the final classification mappings, and five CNN layers with 22 kernels and LeakyReLU activations. Seven outcomes in the final deep network correspond to the classes taken into account: good health, grounded glassy opacity, micro nodules, standardisation, water supply systems, deformation, and a mixture of Aspects. This work used a sample of 14696 input images, obtained over 120 Computed tomography clinics, to train and test the CNN. This is the first deep Network created specifically for the issue. The efficiency of the utilised CNN in comparison to earlier techniques on a difficult collection was demonstrated by a similar evaluation. The classification results of Convolutional in evaluating respiratory signals (around 85.5 percentages) showed its potential. However, the work cannot involve CNN by expanding 3-dimensional data from Computed tomography volume scans and incorporating the utilised approach into a Computer aided system which helps radiologists by providing a differential diagnosis for Lung lesions. This study uses a limited dataset to evaluate the model, making it unsuitable for use in real-world conditions.

In order to extract relevant images, content-based image retrieval systems thoroughly analyse underlying image LL properties. This eliminates the need for speech recognition tags, textual descriptions, or phrases to be connected with the images. For resemblance identification and classification for a particular query image, a CBIR system preserves great image visualisations in the form of extracted features. The initial identification and categorization of lung disorders depending

on lung X-ray images are made possible by the CBIR system for the recovery of medical images suggested in the paper [14].Balancing across several measurement approaches, extensive experiments on the benchmark dataset showed that the strategy improved precision by 49.7 %. Additionally, the area under the precision-recall curve values for all subclasses showed a 26.6 % enhancement. Due to its numerous levels and lengthy training period, this strategy is ineffective.

An intriguing development is the use of AI in the identification of chronic obstructive pulmonary disorders. Discovering commonalities in forensic test data allows AI systems to anticipate health outcomes or identify obstructionist traits. However, prospects for AI in the identification of acute respiratory disorders and to summarise recent trends has to be evaluated. The paper [11] provide an explanation for the use of AI in telehealth, breath research, lung sound assessment, and other management of cancer. By offering precise differentiated diagnosis, ML has yielded promising result in computerized pulmonary function interpretation. Modern DL models for obstructive classification tasks in Computed tomography include Convolutional neural network. Due of the extensive time and resource requirements, this approach is ineffective.

The paper [15] used a novel hybrid DL framework called VDSNet for the detection of lung illnesses in X-ray images. A database of National institutes of health chest X-ray images obtained from the Kaggle source is used for the assessment. The overall recognition accuracy for the full dataset is 73percentage points for VDSNet, whereas the maximum accuracy for natural grey, vanilla Color images, hybrid Neural VGG, basic CapsNet, and customized CapsNet are 68%, 69%, 69.4%, 61%, and 64%, respectively. VDSNet has a validation accuracy value of 73%, which is higher than the reference dataset's accuracy score of 71%. However, instead of 19 seconds for the measurement, VDSNet takes a time for training of 431 seconds for the whole data source. However, computerized chest X-ray diagnostic techniques is not enhanced in this work, so this paper focuses on the application of image data enhancement techniques such as colour space implants, kernel filtering, deep feature improvements, etc. The VDSNet approach can be used to analyse X-ray images of potential patients and healthy controls for the individuals who have pneumonia associated with COVID-19. When focusing on the large-scale dataset, this study research meets certain difficulties. Smaller datasets can therefore produce good accuracy, but they are ineffective for use in real-world scenarios.

An automatically generated method for the recognition and classification of ILD patterns is provided in the paper [16]. It is done by removing designs for the modest inter-class information variability and large intra-class value fluctuation by the use of translational and luminance effects, respectively. The Template-Matching Combined Sparse Coding approach is a brand-new and effective dimensionality reduction technique that differs substantially from defined areas of interest inside lung parenchyma that are resistant to translational and illuminating changes. Using a framework comparison procedure, the converted image patches is matched to all potential models of the image. By minimising the objective function of the classification model between the translation enhanced image and the reference, the equivalent sparse matrices for the set of translation texture features and their corresponding framework are produced. For handling high-intra class characteristic variability challenges, a SVM is created, which improves classification performance. In this work, zone of interests of 5 lung tissue patterns - healthy, emphysematous, surface - are found and used. These designs were chosen from an internally multimedia record that includes high-resolution positron emission tomography image series. The method works more effectively than the majority of cutting-edge multi-class classification methods. Whenever the data set includes greater amounts of noise, it fails to function as well.

In the paper [17], authors classified lung HRCT extracted features into five classes: good material, emphysema, field glass, fibrosis, and micronodules using an enhanced Dense-Net algorithm with small kernel DenseNet. The SK-design DenseNet's consists of two compact blocks and two different levels. Each thick block has six groups in it. The SK-DenseNet model is more efficient for extracting high level and minor pathologic information for ILD categorization utilising a convolution kernel in accordance with the properties of Computed tomography features of respiratory disease. According to experimental findings, the SK-DenseNet performed best than other Convolutional networks like DenseNet, AlexNet, VGGNet, and ResNet. However, iterations of the research will concentrate on images with ILD patter annotations. This method is not effective since the Indirect effects of hMIKO-1 on T and B cells and other cells of inflammation are also possible. Table I depicts the comparison of existing approaches' merit and demerits.

In an animal model of bleomycin-induced ILD, the paper sought to determine how the hybrid proteins known as human MIKO-1 affected murine macrophages activity and whether it had any protective effects. In order to do this, the phenotype of hMIKO-1-co-cultured thioglycolate-induced murine intraperitoneal lymphocyte was investigated. Since day 0 to day 14, mice were divided into regular and given different doses. Since day 28, the mice were put to death, and the organs are examined for collagen fibres, and for levels of gene transcription. In vitro, hMIKO-1 prevented murine macrophage from polarising toward an M2 preponderance [18]. In comparison to the BLM-alone category, the histologic grade of the lung pathology and the lung extracellular matrix components level were drastically decreased in the BLM + hMIKO-1 collective. This strategy is inappropriate for delivering a greater accuracy level.

TABLE I. COMPARISON OF EXISTING APPROACH MERIT AND DEMERITS

References	Method	Implementation	Advantage	Disadvantage
[13]	CNN	Python language	With no data loss, it lowers the considerable dimensionality of images.	This study uses a limited dataset to evaluate the model, making it unsuitable for use in real-world conditions
[14]	CNN	Python and MATLAB	It requires less work from humans to create its functions.	Due to its numerous levels and lengthy training period, this strategy is ineffective.
[11]	AI	PFT interpretation software	It can considerably boost accuracy while reducing errors.	Due of the extensive time and resource requirements, this approach is ineffective.
[15]	VDSNet	Tensorflow, Jupyter Notebook, and Keras	Much less time is needed for training.	When focusing on the large-scale dataset, this study research meets certain difficulties. Smaller datasets can therefore produce good accuracy, but they are ineffective for use in real-world scenarios.
[16]	B-MCSVM	-	It uses relatively little storage and performs well in high-dimensional areas.	Whenever the data set includes greater amounts of noise, it fails to function as well.
[17]	SK-DenseNet	GraphPad Prism version 7.0 software	It has more effectively utilized features	This method is not effective since the Indirect effects of hMIKO-1 on T and B cells and other cells of inflammation are also possible.
[18]	PSO and Fuzzy C-mean Clustering method	Python coding	In terms of processing efficiency, it is better in terms of speed and memory needs.	This strategy is inappropriate for delivering a greater accuracy level.

III. DATASET

Among the main obstacles to the development of DL in medical image analysis is the absence of enough training data, which are necessary to establish the accuracy of DL classifiers. The production of huge medical imaging datasets is difficult due to the annotation calls for a lot of input from medical professionals. In particular, several expert perspectives are needed to address the issue of human error. The collection includes medical information from patients with pathologically confirmed classifications of ILDs as well as high-resolution computerized tomography image series with 3-dimensional identified areas of diseased lung tissue. The goal of this effort is to make up for the dearth of publicly accessible datasets of ILD cases that may be used as a foundation for the creation and assessment of image-based computerised diagnostic tools. The present research makes use of the freely accessible MedGIFT database [19]. The database contains 108 HRCT images with annotations. It has 17 distinct ILD designs, each measuring 512 × 512. A complete set of 1946 ROIs was offered from 108 HRCT imaging series. Five of the most common healthy and ILD patterns are taken into consideration in the present study. Since the database is multipattern, there is a chance that many patterns will coexist in a single slice.

IV. METHODOLOGY

The feature extraction phase of image recognition is crucial. A hybrid spider monkey and lion method is used for feature extraction, and RNN is used for classification. It is used to categorise the diseased portion of the lung for future prevention and find the fastest way for the infected region recognition utilising the distinctive hunting behaviour of lion and monkey. Fig. 1 represents the process of ILD prediction.

The basic process flow diagram for the steps of ILD prediction is shown in Fig. 1. The lung input image is first pre-processed, and then features are retrieved using a combination of lion and spider monkey optimization. RNN was finally utilized to categorise the results.

A. Pre-processing

Pre-processing comes after the images has been chosen as the starting point for ILD diagnosis. The median filter has been used to improve the Lung images by reducing noise and removing unwanted items. A non-linear, well-organized simple image processing method called the median filter is frequently employed to lower noise in images. The result of the Median filter is given by Eq. (1).

$$\hat{g}(x,y) = median_{(a,b)\in T_{xy}}\{f(a,b)\} \quad (1)$$

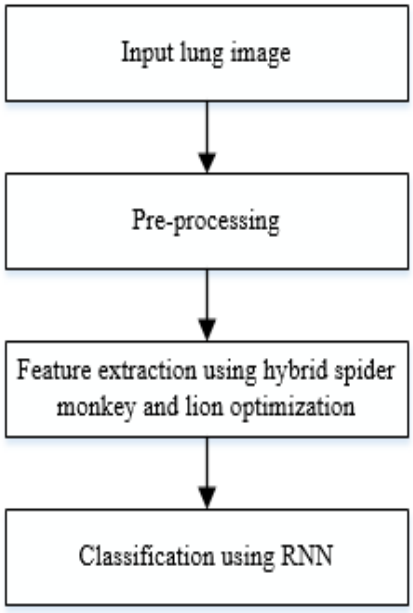

Fig. 1. Process of ILD prediction.

For the goal of detecting arrhythmias, segmentation is the most crucial topic in informatics and the health industry. The main aim of this study is to create and build a reliable classification method using a RNN classifier that is SM and lion-based. Data pre- processing, image segmentation, extraction of features, and classification are the 4 stages of the heartbeat detection algorithm. The standard will be eliminated from the ECG signal when it first enters the information processing phase. The pre-processed sensor will go through the classification step, which will execute the segmentation using the Frequency response. The segmented data move on to the feature extraction phase, where features including wave features and temporal features will be recovered. Pre-processing the information is important since it helps to remove the signal's undesirable components, ensuring that the characteristics that are recovered are correct and suitable for blood pressure and heart rate identification. The retrieved characteristics will be sent to the classification stage, where the Spider Monkey and lion -based Recurrent neural network will be used to classify the disease (RNN classifier).

The hybrid Spider Monkey lion algorithm, which combines the Spider Monkey Optimization (SMO) and the lion algorithms, will be used in conjunction with the RNN in the suggested method. The Lion algorithm is a generalisation of interaction and the activities of lion whereas the SMO leverages the foraging behaviour of spider monkeys in a fission-fusion like framework to address the optimization model. Additionally, combining SMO with lion effectively captures the hunting and intellectual behaviour of the lion. The goal of the optimization ensures that the RNN is effectively tuned for precise predicting and classifying. The suggested method will be put into practise using the MATLAB tool, and its performance will be assessed using metrics like accuracy and excellent put. As a result, when compared to the current strategies, such as DL approach, hierarchical categorization, and research driven technique, the suggested strategy successfully performs the ILD classification and will achieve superior accurateness and excellent output.

B. SMO

A recently introduced stochastic improved algorithm called Spider Monkey Optimization takes its cues from nature. A kind of monkey that is included in the group of creatures that have a fusion and fission social structure is referred to as "spider money." These spider monkeys are frequently observed in groups and have skilled hunting habits. They facilitate food gathering in a variety of ways by sharing pertinent information with the other group members [20]. The advanced food-seeking strategy used by spider monkeys served as motivation for the invention of this SMO method. Fitness function is given in Eq. (2).

$$fitness\ function\ (Fi) = \begin{cases} \frac{1}{1+F_i} & if\ F_i \geq 0 \\ 1 + xyt(F_i), & if\ F_i < 0 \end{cases} \quad (2)$$

Six distinct aspects of the numerical method of SMO foraging behaviour for optimization techniques are covered in the subsequent subsections. SMO first creates a population of N spider monkeys at random. Each S_{ij} in SMO has the following initialization which is shown in Eq. (3).

$$S_{ij} = S_{minj} + X(0,1) \times \left(S_{maxj} - S_{minj}\right) \quad (3)$$

Where S_{minj} and S_{maxj} are lower and upper bounds in jth direction for S_i and $X(0,1)$ denotes a random number in the range [0, 1]. The next section describes all six phases of SMO in detail.

1) Local Leader Phase (LLP): In this step, a current hire for a service user is obtained utilising the information provided by the group members via Eq. (4) and the local leader. The fitness value of the solution determines its excellence. The following iteration will focus on the option with the highest fitness (the new location is preferable to the existing position).

$$S_{newij} = S_{ij} + X(0,1) \times \left(SL_{pj} - S_{ij}\right) + X(-1,1) \times \left(S_{qj} - S_{ij}\right) \quad (4)$$

Where, S_{pj} and S_{qj} denote the positions local group leader and randomly chosen q^{th} spider monkey respectively.

2) Global Leader Phase (GLP): During GLP, each member updates their standpoint depending on knowledge from the firm's global leader and all members, as stated in Eq. (5).

$$S_{newij} = S_{ij} + X(0,1) \times \left(SG_j - S_{ij}\right) + X(-1,1) \times \left(S_{qj} - S_{ij}\right) \quad (5)$$

Where, SG_j shows the jth direction of the global leader. Furthermore, the fitness values is expressed in Eq. (6).

$$P = \frac{fitness_i}{\sum_{i=1}^{K} fitness_i} \quad (6)$$

Similar to LLP, further processing uses the better solution from the newly created position and the old position of the SM.

3) Global Leader Learning (GLL) phase: In this stage, the global leader takes the role with the consistent top fitness, and a global limitation monitor is used to track changes in the role of the global leader.

4) Local Leader Learning (LLL) phase: Local leader is given the necessarily lead with the best fitness. Similar to the GLL phase, the local limitation counter is incremented by one if the new position of the local leader is like the information and establishing.

5) Local Leader Decision (LLD) phase: When a local leader's local limit counter hits a certain count, all group members are reset using Eq. (7).

$$S_{newij} = S_{ij} + X(0,1) \times \left(GL_j - S_{ij}\right) + X(-1,1) \times \left(S_{qj} - S_{ij}\right) \quad (7)$$

6) Global Leader Decision (GLD) phase: If the global leader location is not changed after a certain amount of iterations, it forms tiny size of subcategories. Each group's local leaders in GLD are chosen through the LLL procedure. If the global leader's position is not changed by a

predetermined threshold, all subgroups are combined into one group. SMO imitates the FFS organization in this manner.

C. Lion Optimization Algorithm

Analysing the behaviour of the lion, the computational solution for the Lion optimization method was developed. Hunting, running away to safety, straying, mating, migrating, defending, population stability, and convergence are examples of animal behaviours [21]. Such characteristics are expressed mathematically, and an efficient method is developed. The initial communities are produced using lions, an entirely arbitrary solution. The additional lions are randomly separated into P pride subdivisions, with S percentage of the prides being declared a female lion. Norm's lions are picked as the original population N. The optimum place for each lion is described as the best explanation from previous iterations and it is constantly altered throughout the optimization process. Each lion's ideal place can be found in the proud territory.

Young boys who reach sexual maturity are separated from their parents' dignity and go on to remain nomads, where they have less power than regular males. A nomad lion roams the searching area aimlessly in search of a better location (solution). A powerful nomad male forces the resident male out of the prides when they engage in combat. The regional male lion will take the spot of the nomads' male. Female desert lions occasionally join prides, while other nomadic female lions occasionally leave them. The lesser lion will be mercilessly killed for a number of reasons, including malnutrition and intensity of competition.

The inhabitants in the global optimum were first created spontaneously by the LOA. It observed each distinct solution as a "lion." A lion is described as follows for an Nv multidimensional optimization method which is shown in Eq. (8).

$$Lion = x_1 + x_2 + x_3 + \cdots x_{Nv} \qquad (8)$$

And the assessment of the minimization problem, as shown below, determines the cost (each lion's fitness value) which is shown in Eq. (9).

$$fitness\ value\ of lion = f(lion) = f(x_1 + x_2 + x_3 + \cdots x_{Nv}) \qquad (9)$$

The N pop alternatives were developed primarily at random in the problem space. A random selection of % N options was chosen as NL. P prides were created from the remnant population. Throughout the optimization process, a certain sexual identity was constant for each response in the LOA. In each pride, roughly 75–90 percent of total of the estimated workforce created in the preceding stage were referred to as female lions, with the remaining lions being male, to mimic this nature. Each lion identified its most frequented place while searching. Each pride built its region based on the regions that had been indicated. As a consequence, each pride's region was created by its supporters marking certain sites.

1) Hunting: A specific number of females search for food source in a team in each and every P to provide food for the other P individuals. To surround and capture their food source, these hunting lions employ certain tactics. Typically, as lions hunt, they stick to a same routine. Every lioness changes her hunting position based on where she is and where the other lionesses are. As a result, some hunter lions rotate their prey and assault it from the other direction, and LOA employs opposition-based learning. In Eq. (10) hunter equation is expanded. Three "wings" of hunters are established. The centre wing has the best overall fitness, whereas the left and right wings are determined at random. The prey flees to a new area during a search as the predator gets fitter.

$$hunter = \begin{cases} rand((2 \times PY - hunter, PY), \\ (2 \times PY - hunter) \\ \text{rand } ((2\ \times\ \text{PY} - \text{Hunter}, \text{PY}), \\ (2\ \times\ \text{PY} - \text{Hunter}) <\ \text{PY} \end{cases} \qquad (10)$$

D. Hybrid Spider Monkey and Lion Optimization

For particular jobs, it has been demonstrated that the SMO system integrates more quickly than alternative techniques. As a result, it can decelerate down as it approached the global ideal point. The probability of becoming trapped in the region of local optima rises as the algorithm continuously incorporates with the world wide optimal position. The SMO algorithm's dependency on search parameters seems to be another flaw. Based on the choices made, the accumulation rates may change. The SMO approach has undergone several modifications to increase its efficacy, with the main goal of balancing the incremental and radical features. Among the suggestions are tweaks to the developmental technique, adjustments to the parameters, adjustments to the upgraded criteria, and the introduction of better developing methods. It has been demonstrated that the lion is more efficient and has a better rate of success in multipurpose scenarios than the SMO, despite the fact that the lion's algorithms does not take acceleration into account. The flow diagram for the proposed method is given in Fig. 2.

$$fitness\ function\ (Fi) = \begin{cases} \frac{1}{1+f(x_1+x_2+x_3+\cdots x_{Nv})} & if\ \ F_i \geq 0 \\ 1 + xyt(f(x_1 + x_2 + x_3 + \cdots x_{Nv})),\ if\ F_i < 0 \end{cases} \qquad (11)$$

The process flow diagram for the hybrid spider monkey and lion optimization is shown in Fig. 2. When features are successfully extracted from ILD images, the fitness value is calculated.

E. Recurrent Neural Networks

The foundation of NN topologies is the idea that all signals are consecutively redundant. However, this presumption is erroneous and might be harmful for many applications, like time report and natural language processing where the relationships among successive training instances are crucial. A type of artificial neural network known as an RNN adds loops to the feed - forward neural network to increase its functionality. A recurrent hidden state, whose activation at each step depends on that of the preceding step, allows an RNN, unlike a feed - forward neural network, to process the complex combination. The system can display variable

temporal behaviour in this way. Fig. 3 depicts the basic structure of RNN.

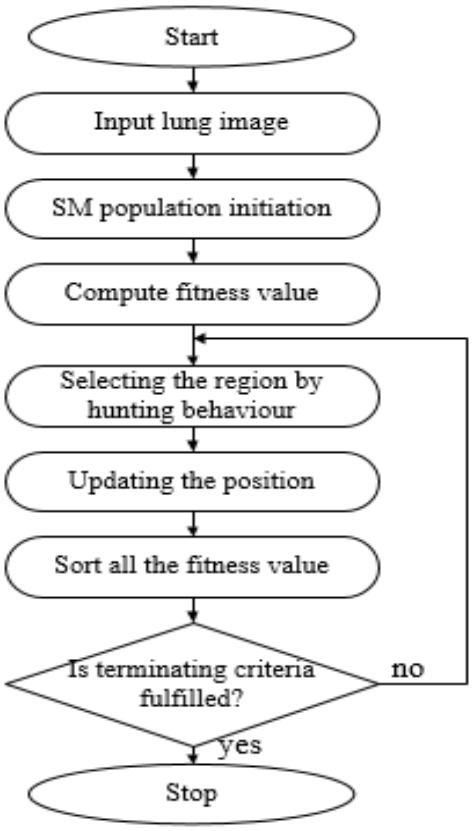

Fig. 2. Flow diagram for the proposed method.

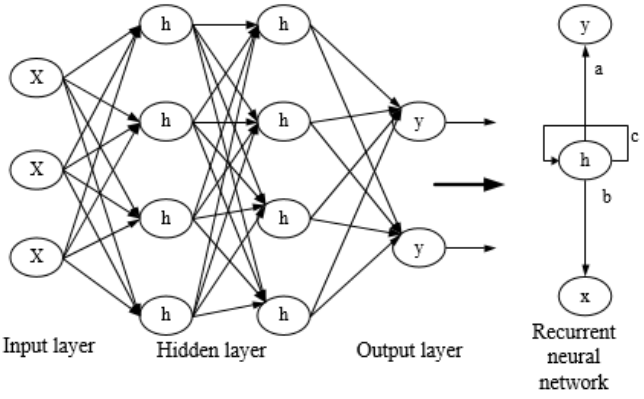

Fig. 3. Working process of RNN.

Fig. 3 depicts the fundamental layout of an RNN. Input, hidden, and output layers are all three layers. The ILD image results are successfully classified by using this approach.

V. Result and Discussion

Utilizing the images of the gathered plant leaves, the suggested strategy has been evaluated. To distinguish the diseased lung from the healthy lung, the suggested method employed hybrid spider monkey and lion optimization with recurrent neural network. The study assesses the 4 commonly used evaluation metrics, including classification accuracy, precision, recall, and F1-score, which are described below.

With regard to the lung images that are obtainable, accuracy produces suitable results. In Eq. (12), accuracy is represented.

$$Accuracy = \frac{TN+TP}{FN+FP+TP+TN} \quad (12)$$

Precision thoroughly assesses a classifier's performance. Precision will be high if the lung image has low positives and low positives if the lung image has high positives. In Eq. (13) precision is represented.

$$precision = \frac{TP}{FP+TP} \quad (13)$$

Recall gauges how complete the classification is. More positive samples are found greater the recall. The Eq. (14) contains a representation of the recall formula.

$$Recall = \frac{TP}{FN+TP} \quad (14)$$

The F1-score measurement combines precision and recall. The F1-score measure is determined by calculating from the recognition rate. Eq. (15) represents the F1 measure.

$$F1 - score = \frac{2 \times Precision \times Recall}{Precision+Recall} \quad (15)$$

From Table II, the accuracy of the proposed system is 99.8% which is high compared to other existing approaches such as ACO is 98.6%, CNN is 98.97% and SMB is 97%.

The existing and proposed analyses for accuracy measurements were compared in Table II and Fig. 4 represents the graph of accuracy measure, the suggested hybrid spider monkey and lion obtained more effective results.

The existing and proposed analyses for precision measurements were compared in Table II and Fig. 5 represents the graph of precision measure, the suggested hybrid spider monkey and lion obtained more effective results.

The existing and proposed analyses for recall measurements were compared in Table II and Fig. 6 represents the graph of recall measure, the suggested hybrid spider monkey and lion obtained more effective results.

The existing and proposed analyses for F1-score measurements were compared in Table II and Fig. 7 represents the graph of accuracy measure, the suggested hybrid spider monkey and lion obtained more effective results.

TABLE II. Performance Comparison Matrix

Method	Accuracy	Precision	Recall	F1-score
ACO	98.6 %	96%	96%	97.6%
CNN	98.97%	98.3%	98.7%	98.7%
SMB	97%	96%	97%	96%
Hybrid spider monkey and lion	99.8%	99.9%	99.7%	99.89%

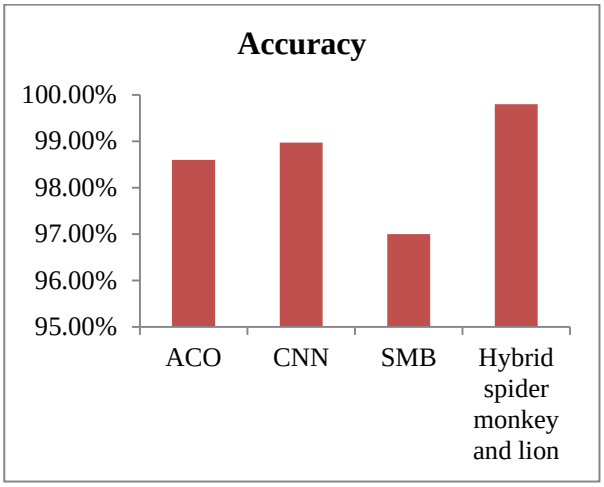

Fig. 4. Graph of accuracy measure.

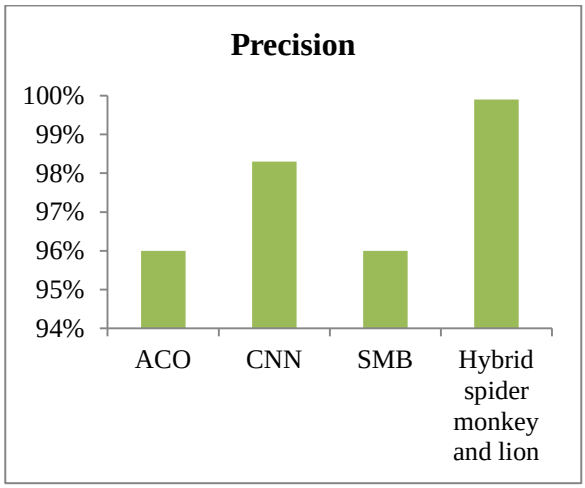

Fig. 5. Graph of precision measure.

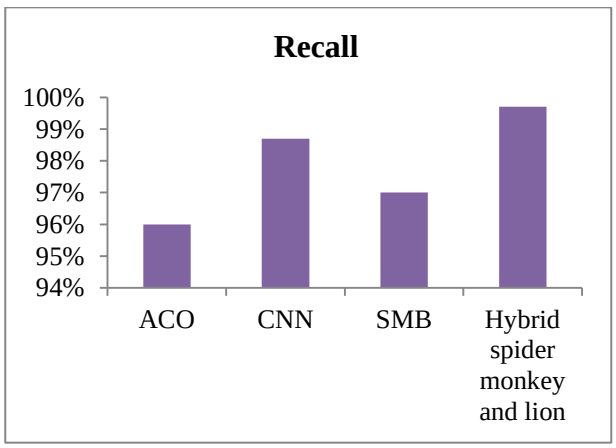

Fig. 6. Graph of recall measure.

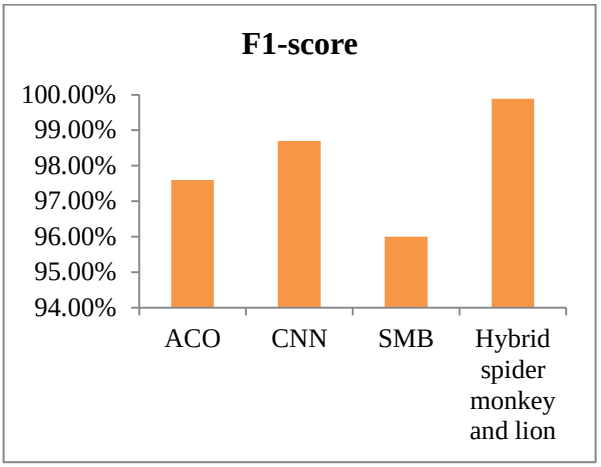

Fig. 7. Graph of F1-score measure.

In this instance, the hybrid spider monkey and lion with RNN model outperformed the ACO, CNN, and SMB models. The accuracy percentages for ACO, CNN, and SMB are 98.6%, 98.97%, and 97%, respectively. Precision, recall, and F1-score have better rates in the hybrid spider monkey and lion method compared to other models, and the F1-score has attained the greatest rate compared to other models due to the accuracy rate of 99.8% in the hybrid spider monkey and lion model.

VI. Conclusion

Deep learning (DL), which has significantly outperformed more conventional ML algorithms in recent decades, has taken centre stage in the mechanization of our daily lives. DL -based apps will replace humans in some roles, and autonomous robots will handle the majority of everyday chores. In contrast to other real-world issues, DL is just slowly making its way into the healthcare industry, particularly in the field of medical imaging. It has been suggested to use full HRCT images in a two-stage hybrid deep learning network screening method for interstitial lung disease (ILD). The accuracy, precision, recall, and F1 measure are determined by the suggested approach. The developed method yields a high prediction accuracy of 99.8%, and the proposed model is subsequently used for medical diagnostics. In this study, the IL disease prediction system is based on an improved spider monkey and lion optimization with RNN. The feature extraction was done with hybrid spider monkey and lion optimization, while the classification was done with RNN classifier. The proposed approach is utilized to distinguish between diseased and healthy Lung. With maximum accuracy of 98.8%, precision of 99.9%, recall of 99.7%, and F1-score of 99.89%, the suggested spider monkey and lion optimization with RNN is better than the existing approaches. Future research will build on this work by attempting to forecast the incidence of other serious illnesses including cancer and other heart-related diseases with high computational speed.

REFERENCES

[1] J. Ker, L. Wang, J. Rao, and T. Lim, "Deep Learning Applications in Medical Image Analysis," IEEE Access, vol. 6, pp. 9375–9389, 2018, doi: 10.1109/ACCESS.2017.2788044.

[2] B. Zhou, B. J. Bartholmai, S. Kalra, and X. Zhang, "Predicting lung mass density of patients with interstitial lung disease and healthy subjects using deep neural network and lung ultrasound surface wave elastography," J. Mech. Behav. Biomed. Mater., vol. 104, p. 103682, Apr. 2020, doi: 10.1016/j.jmbbm.2020.103682.

[3] G. Litjens et al., "A survey on deep learning in medical image analysis," Med. Image Anal., vol. 42, pp. 60–88, Dec. 2017, doi: 10.1016/j.media.2017.07.005.

[4] D. Bermejo-Pelamp, "Classification of Interstitial Lung Abnormality Patterns with an Ensemble of Deep Convolutional Neural Networks" Scientific Reports, 2020.

[5] M. I. Razzak, S. Naz, and A. Zaib, "Deep Learning for Medical Image Processing: Overview, Challenges and the Future" 2018.

[6] A. Nyma, M. Kang, Y.-K. Kwon, C.-H. Kim, and J.-M. Kim, "A Hybrid Technique for Medical Image Segmentation," J. Biomed. Biotechnol., vol. 2012, pp. 1–7, 2012, doi: 10.1155/2012/830252.

[7] M. L. Smith, "The histologic diagnosis of usual interstitial pneumonia of idiopathic pulmonary fibrosis. Where we are and where we need to go," Mod. Pathol., 2022.

[8] R. Borie et al., "The genetics of interstitial lung diseases," Eur. Respir. Rev., vol. 28, no. 153, p. 190053, Sep. 2019, doi: 10.1183/16000617.0053-2019.

[9] E. Bendstrup, J. Møller, S. Kronborg-White, T. S. Prior, and C. Hyldgaard, "Interstitial Lung Disease in Rheumatoid Arthritis Remains a Challenge for Clinicians," J. Clin. Med., vol. 8, no. 12, p. 2038, Nov. 2019, doi: 10.3390/jcm8122038.

[10] P. Hattikatti, "Texture based interstitial lung disease detection using convolutional neural network," in 2017 International Conference on Big Data, IoT and Data Science (BID), Pune, India: IEEE, Dec. 2017, pp. 18–22. doi: 10.1109/BID.2017.8336567.

[11] N. Das, M. Topalovic, and W. Janssens, "Artificial intelligence in diagnosis of obstructive lung disease: current status and future potential," Curr. Opin. Pulm. Med., vol. 24, no. 2, pp. 117–123, Mar. 2018, doi: 10.1097/MCP.0000000000000459.

[12] S. P. Pawar and S. N. Talbar, "Two-Stage Hybrid Approach of Deep Learning Networks for Interstitial Lung Disease Classification," BioMed Res. Int., vol. 2022, pp. 1–10, Feb. 2022, doi: 10.1155/2022/7340902.

[13] S. Agrawal, A. Chowdhary, S. Agarwala, V. Mayya, and S. Kamath S., "Content-based medical image retrieval system for lung diseases using deep CNNs," Int. J. Inf. Technol., vol. 14, no. 7, pp. 3619–3627, Dec. 2022, doi: 10.1007/s41870-022-01007-7.

[14] M. Anthimopoulos, A. Christe, and S. Mougiakakou, "Lung Pattern Classification for Interstitial Lung Diseases Using a Deep Convolutional Neural Network," 2015.

[15] S. Bharati, P. Podder, and M. R. H. Mondal, "Hybrid deep learning for detecting lung diseases from X-ray images," Inform. Med. Unlocked, vol. 20, p. 100391, 2020, doi: 10.1016/j.imu.2020.100391.

[16] C. Helen Sulochana and S. Praylin Selva Blessy, "Interstitial lung disease detection using template matching combined sparse coding and blended multi class support vector machine," Proc. Inst. Mech. Eng. [H], vol. 236, no. 10, pp. 1492–1501, 2022.

[17] T. Kotani, M. Ikemoto, S. Matsuda, R. Masutani, and T. Takeuchi, "Human MIKO-1, a Hybrid Protein That Regulates Macrophage Function, Suppresses Lung Fibrosis in a Mouse Model of Bleomycin-Induced Interstitial Lung Disease," Int J Mol Sci, 2022.

[18] P. Kavitha and S. Prabakaran, "A Novel Hybrid Segmentation Method with Particle Swarm Optimization and Fuzzy C-Mean Based On Partitioning the Image for Detecting Lung Cancer," 2019.

[19] A. Depeursinge, A. Vargas, A. Platon, A. Geissbuhler, P.-A. Poletti, and H. Müller, "Building a reference multimedia database for interstitial lung diseases," Comput. Med. Imaging Graph., vol. 36, no. 3, pp. 227–238, 2012, doi: https://doi.org/10.1016/j.compmedimag.2011.07.003.

[20] H. Sharma, G. Hazrati, and J. C. Bansal, "Spider Monkey Optimization Algorithm" 2019.

[21] M. Selvi, "Lion optimization algorithm (LOA)-based reliable emergency message broadcasting system in VANET" 2020.